Numerical Study of Contra-Rotating Vertical Axis Wind Turbine H-Rotor Darrieus Type

Aditya Ilham Setyawan Haryogo
Postgraduate Study, Department of Mechanical Engineering,
Institut Teknologi Sepuluh Nompember, Sukolilo, Surabaya 60111,
INDONESIA

Vivien S. Djanali[*]
Department of Mechanical Engineering,
Institut Teknologi Sepuluh Nopember,Sukolilo, Surabaya 60111,
INDONESIA
[*]*vivien_s@me.its.ac.id*

Bagus Nugroho
Department of Mechanical Engineering,
The University of Melbourne, Parkville, Victoria, 3010, AUSTRALIA

ABSTRACT

The new Contra-rotating Darrieus turbine configuration has been invented to enhance the Vertical Axis Wind Turbine (VAWT) performance. This configuration increases the relative rotational speed of the generator, resulting in higher output power. It is well known that the increase can reach four times the output power. However, how the Darrieus turbine VAWT contra-rotating configuration influences its aerodynamic performance still needs to be discovered. This study investigates the aerodynamic performance of the contra-rotating configuration by comparing it to the single-rotating Darrieus turbine VAWT under the same conditions. The freestream speed is 5 m/s, with TSR varying from one to two intervals of 0.2. This research is being completed using Computational Fluid Dynamics (CFD) 3D cases with an Unsteady Reynold Average Navier-Stokes (URANS) equation as the turbulent model equation. The results of this study show that in terms of output power or Power coefficient (Cp), the contra-rotating has a greater value than the single-rotating configuration. However, in all TSR variations, contra-rotating outperforms single-rotating in terms of aerodynamic performance or moment coefficient (Cm). This is due to the fact that the aspect ratio of stage 1 contra-

ISSN 1823-5514, eISSN 2550-164X
Received for review: 2022-08-19
Accepted for publication: 2023-02-28
Published: 2023-04-15

https://doi.org/10.24191/jmeche.v20i2.22050

rotating rotor is lower than the single-rotating rotor, resulting in more significant blade tip losses in contra-rotating. The flow was discovered through the gap between stages 1 and 2 contra-rotating, providing additional momentum. This phenomenon increases Cm at an azimuth angle of 200°-255°.

Keywords: *Darrieus Turbine; Contra-Rotating; Numerical Simulation; Power Coefficient; Moment Coefficient*

Introduction

The development of renewable energy, especially the Vertical Axis Wind Turbine (VAWT), is increasing. due to the awareness of the current pollution levels from the use of fossil energy [1]. VAWT itself has several advantages when compared to Horizontal Axis Wind Turbine (HAWT), such as a simple design so that the costs required are not much, being able to work in urban areas or areas with low wind speeds and being able to work in all different wind directions [2]. However, people still use HAWT more than VAWT because HAWT produces better performance when compared to VAWT and has a better self-start. Many researchers were trying to improve the quality of VAWTs, such as [3]-[4], who import hybrid VAWTs to have good performance and self-start. Bausas and Danao [5] used an airfoil camber to improve the performance of the Darrieus turbine VAWT. Several studies [2], [6]–[8] examined the effect of solidity on tip speed ratio. Li et al. [9] examined the effect of aspect ratio on turbine performance. Zhu et al. [10] investigated the addition of a flap. Liu et al. [11] investigated the effect of the trailing edge movable flap on the VAWT performance of the Darrieus turbine. Several studies from [12]-[16] examined the effect of pitch angle on VAWT performance. Azizuddin et al. [17] studied VAWT with a novel blade design.

Didane et al. [18] conducted an experiment using a new rotor configuration, namely the contra-rotating VAWT, especially with the Darrieus turbine. This configuration has two rotors with the same airfoil type and dimensions rotating in opposite directions but having one axis of rotation. This configuration is inspired by contra-rotating HAWT where the configuration utilizes the residual wind speed from the main rotor by using an additional rotor located behind the main rotor so that the turbine's performance can be increased. The incoming wind speed in the contra-rotating either through the first stage or the second stage has the same magnitude, so the moment was greater than just the first stage. In contra-rotating, both the rotor and stator at the generator rotated in opposite directions, so it produced a higher relative rotation. This configuration used a semi-cylindrical pipe placed on the connector between the rotor and the shaft to assist in self-starting. This configuration did not require an electric motor as a helper in self-starting, so the tip speed ratio used can be less than one. That study stated the increasing

Coefficient Performance (C_P) with contra-rotating configuration up to 40% compared to the single-rotating. Contra-rotating VAWT produced a greater moment than single-rotating VAWT. Therefore, the contra-rotating effect on the Darrieus turbine performance can significantly increase the turbine performance. After following this study, there came researcher research this configuration, such as examining the concept of contra-rotating VAWT using a Savonius turbine conducted by Ahmudiarto et al. [19]. From this study, it was found that the performance obtained increased up to two times. Didane et al. [20] also conducted research on contra-rotating using a Savonius turbine. The three blades of Savonius were tested in a wind tunnel within an inlet velocity of 2 m/s up to 9 m/s. The best results were obtained at low wind speeds (2 m/s), with an average Cm increasing up to 42% and Cp 28% for contra-rotating configuration. Then the research was conducted by Didane et al. [21] to determine the effect of axial distance and aspect ratio. The study found that the best performance was obtained by using the smallest axial distance and the largest aspect ratio. Didane et al. [22] also studied using Savonius and Darrieus turbines in the contra-rotating VAWT configuration with low wind speed starting from 2 m/s to 9 m/s. it was found that contra-rotating increased the efficiency system by up to 42%. Particularly, the Darrieus turbine resulted in a higher efficiency along with the increasing wind speed. While in the savonius turbine, the efficiency was opposite with the Darrieus turbine.

Jung et al. [23] investigated contra-rotating HAWT with optimal variations in axial distance and diameter size of the auxiliary rotor. The best performance is discovered in the size and axial distance, which is at 12 of the main rotor diameters. Ko et al. [24] conducted a numerical study of contra-rotating using a Darrieus turbine. This study adopted the contra-rotating geometry from [18], with variations of thickness airfoil, camber airfoil, and also the axial distance between the first stage and the second stage. The tip speed ratio value was conditioned as same as in [18]. this study aimed at the effect of contra-rotating without semi-cylindrical pipes that connected the rotor's shaft with the performance. The results showed that the greatest thickness can produce better performance. In contrast, airfoils with the largest camber can produce the best performance. However, this study resulted in a very small C_P compared to the research conducted by Didane at the same tip speed ratio value.

Previous studies [18], [24] showed that contra-rotating Darrieus turbines were still limited to a low tip speed ratio which was below one while this tip speed ratio was not an ideal condition for Darrieus turbine working on [22]. Therefore, the aerodynamic performance characteristic of the configuration was yet to be explained. This study aims to determine the effect of the contra-rotating VAWT configuration on the Darrieus turbine with an ideal tip speed ratio for the Darrieus turbine working using Computational Fluid dynamics (CFD). This study uses the three-dimensional unsteady simulation case to obtain more accurate results and representation of the three-

dimensional flow structure across the contra-rotating turbine rotors. To the best of our knowledge, this is the first paper to analyze the flow structure around the contra-rotating turbine and compare it with the single-rotating one.

Method

Turbine configuration

This study used a single-rotating configuration to compare the performance with contra-rotating. This single-rotating configuration followed the turbine model from [28], Darrieus turbine with the H-rotor with a diameter rotor of 0.74 m, rotor height of 0.6 m, airfoil NACA 0015 with a chord length of 0.15 m as shown in Figures 1a and 1d. Meanwhile, the contra-rotating configuration consisted of two stages rotating in opposite directions i.e. the first stage rotated clockwise direction while the second stage rotated counterclockwise direction. This configuration has the same dimensions as single-rotating, only this configuration, was divided into two parts as shown in Figure 1d. based on research from [1], stated that the smallest axial distance gave the best performance. More details are shown in Table 1

Table 1: Details of the single-rotating and contra-rotating turbine

Parameter	Single - Rotating	Contra-Rotating
Diameter, D (m)	0.74	0.74
Radius, R (m)	0.37	0.37
Height, H (m)	0.6	0.3 x 2 stage
Number of Blades, N (m)	3	3 x 2 stage
Chord Length, c (m)	0.15	0.15
Airfoil	NACA 0015	NACA 0015
Pitch Angle (β) (°)	0	0
Aspect Ratio, H/D (-)	0.81	0.405 x 2 stage
Solidity Ratio, σ (-)	0.193	0.193
Re_D (-)	228914.14	228914.14

Numerical method

The three-dimensional simulation was carried out using the finite volume method with the Unsteady Reynold Averaged Navier Stokes (URANS) as the basic flow equation to be solved. The URANS equation has several variables such as time, velocity, pressure, and turbulent properties. The velocity, time, and turbulent properties were solved using a second-order discretization scheme to get good accuracy, while the pressure variable uses a SIMPLE pressure-velocity coupling scheme [26]. The turbulent model used was SST-kw because this turbulent model can capture the phenomenon of flow

separation in the adverse pressure gradient region to provide more accurate results [27].

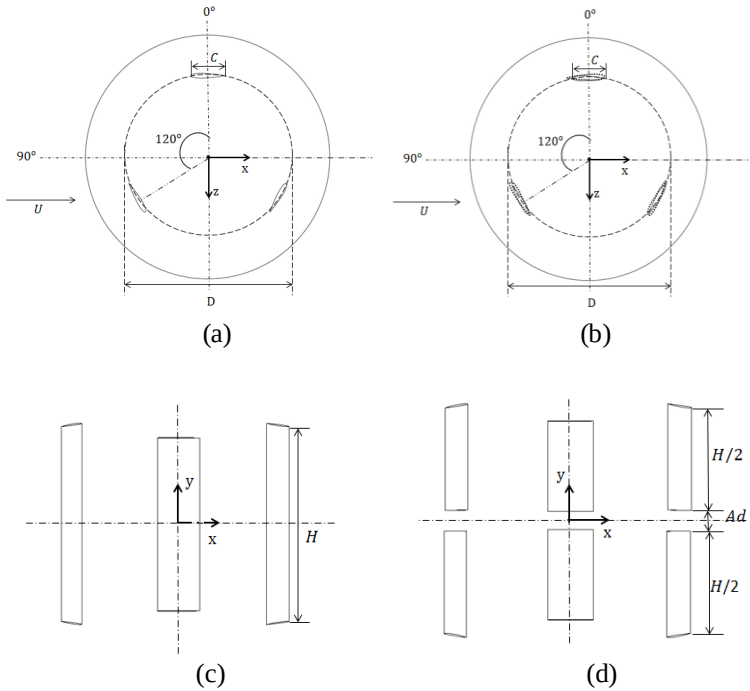

Figure 1: Geometry and dimensions of the contra-rotating Darrieus VAWT turbine; (a) top view single-rotating, (b) top view contra-rotating, (c) side view single-rotating, and (d) side view contra-rotating

The boundary condition used was the velocity inlet with a value of 5 m/s while the outlet used a pressure outlet with a value of 0 pascals. The side wall, the top wall, and the bottom wall used a slip condition wall, but the airfoil used a no-slip condition wall. The cell zone in the fixed zone was set to stationary while the rotating zone was set to rotary with the boundary between the fixed zone and the rotating zone set as an interface so that the two cell zones can communicate. The time step was set using the azimuth angle interval (dθ) of 0.5° so the results obtained are accurate while the computation time is also not too long [26]. As many as 22 revolutions were conducted to obtain accurate and stable results [26]. Therefore, in this study, the simulation was divided into 2 steps. The first step of the simulation was carried out with 20 revolutions with a dθ of 10°. The discretization scheme especially for turbulent properties used first-order and the convergence criteria were set to 10^{-4} for all properties. This simulation aimed to obtain a stable calculation. After that, the simulation

was repeated with 2 revolutions at a dθ of 0.5°. The discretization schemes used all second order, and the convergence criteria were set 10^{-5}. This simulation aimed to get accurate results so that the simulations carried out in this study obtained stable and accurate results.

The domain calculation that was simulated consists of two different cell zones, namely the fixed zone and the rotating zone. There are two rotating zones each on the first stage and the second stage which allows for the rotor to rotate in opposite directions. The length of the calculation domain itself was 25D while the width was 10 D. The height was made of 6D as shown in Figure 2. The dimensions of the calculation domain were determined in such a way that the resulting blockage ratio was not more than 5% whereas the blockage ratio is a ratio between swept area turbine with a cross-sectional area of domain calculation [25].

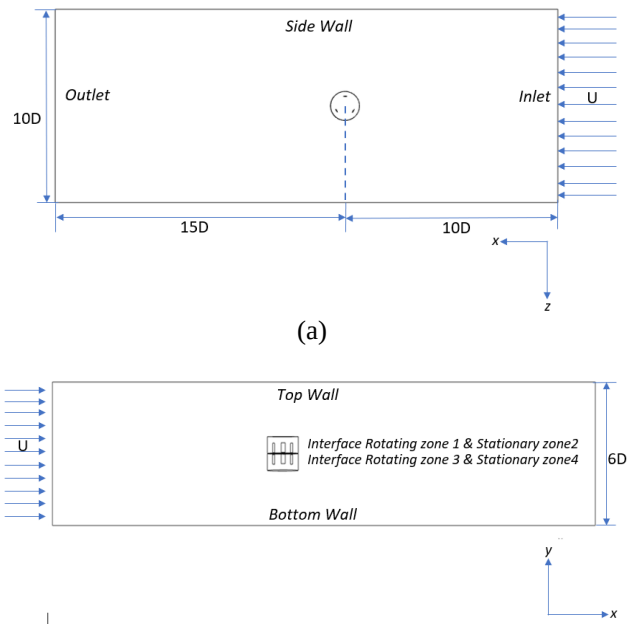

Figure 2: Domain calculation (a) top view, and (b) side view

The mesh that can be applied to the calculated domain can only use a mesh with a tetrahedral mesh. This was because the domain calculation that has been made has a slightly complicated form. The use of tetrahedral mesh was more flexible for complex domain calculations but has a drawback related to accuracy. In addition, using tetrahedral requires a longer process in the simulation than using a hexahedral mesh which will be a problem in this study

because this research relied heavily on high accuracy but with fast computation time. Therefore, it was necessary to make some auxiliary lines in the calculation domain to ensure that a hexahedral mesh dominates the mesh that can be applied to the calculation domain as in Figure 3. Thanks to the helplines provided for the domain calculation, the mesh can be used for the domain calculation using hexahedral. However, for the mesh around the rotating zone, it was very difficult to condition the hexahedral with a structured mesh because the geometry of the Darius turbine was quite complicated. Therefore, auxiliary lines were added around the airfoil so that the mesh around the airfoil can be hexahedral conditioned with a structured mesh. The first distance between the wall of the blade and the first cell was described as y^+. Therefore y^+ was conditioned at $y^+ < 5$ so that the calculation reached the viscous sub-layer area to increase the accuracy.

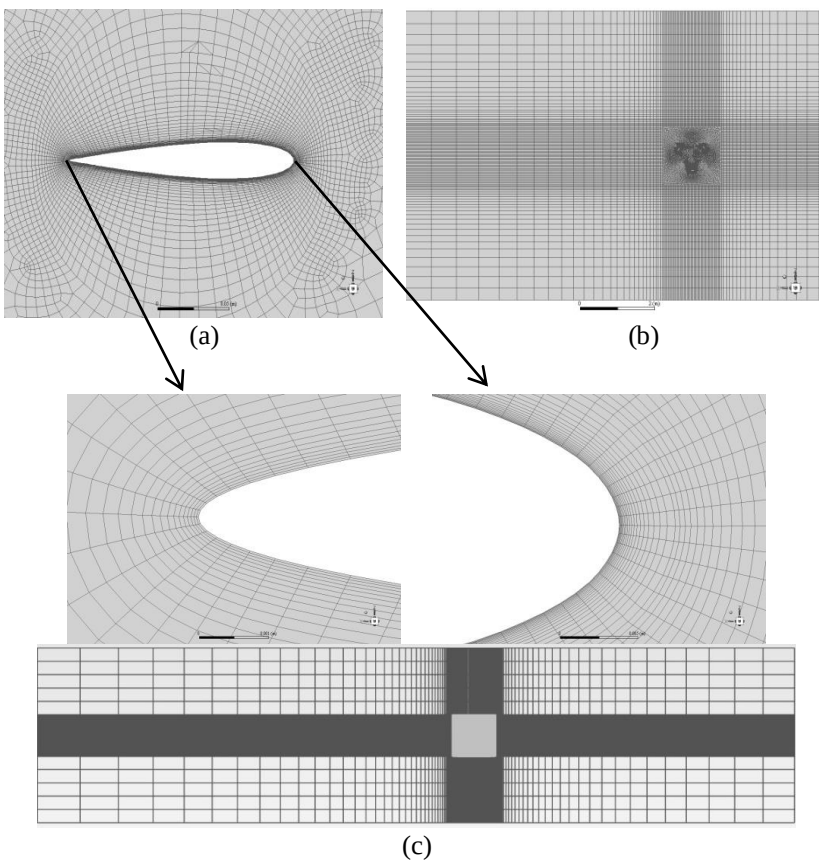

Figure 3: Overall mesh; (a) around the airfoil, (b) top view, and (c) side view

Grid independence test

One of the factors that affect the simulation process's accuracy is the number of cells used. Ideally, the more cells used, the more accurate the simulation results will be.

Table 2: GIT result

Number of cells	Coefficient moment	Maximum y+	Maximum skewness	Relative error coefficient moment
1067739	0.269627	2.042	0.77	-
1393864	0.267208	2.032	0.77	0.008972
1719989	0.264362	2.045	0.75	0.010651
2046114	0.2602057	2.038	0.7	0.0026
2372239	0.260884	2.02	0.7	0.0026

However, with many cells, the computation time will also be longer. Then it is necessary to use the optimal number of cells. Optimal means that by using as few cells as possible, the desired parameter results slightly different from higher cells. A test was carried out namely the Grid independence test (GIT). In this study, it was determined that there were five numbers of cells used, namely 1 million, 1.4 million, 1.7 million, 2 million, and 2.4 million. The parameter to be compared is the mean Coefficient Moment (C_M) for each number of cells produced. In the GIT process, It was used a constant wind speed of 5 m/s with a constant tip speed ratio of 1.4.

From the tests carried out, Table 2 shows that the number of cells of 2 million began to show a small difference in mean C_M. It was found that the number of cells 1 million, 1.4 million, and 1.7 million still produced fluctuations in mean C_M. Therefore, in this study, the number of mesh 2 million was taken as the optimum mesh with maximum y^+ at 2.038.

Governing Equations

Conservation mass and momentum equation

When using the CFD approach to solve problems, two basic equations of flow are used, namely the conservation of mass and momentum. Equation 1 refers to the mass conservation of the fluid flowing in the control volume, in which the dot product of nabla (∇) and the velocity vector ($\vec{V}$) are equal to 0. This implies that the fluid mass flow in the control volume must be constant.

$$\nabla.\vec{V} = 0 \tag{1}$$

Equation 2 depicts the fluid momentum equation when working in volume control with the x coordinate. Due to the turbulent conditions, there are several additional variables ($\overline{u'^2}$, $\overline{u'v'}$, $\overline{u'w'}$) as Reynold Stresses that are resolved in this study. This is known as the Reynold Average Navier Stokes (RANS) equation.

$$\rho\left(\frac{\partial u}{\partial t}+u\frac{\partial u}{\partial x}+v\frac{\partial u}{\partial y}+w\frac{\partial u}{\partial z}\right)=\rho.g-\frac{\partial p}{\partial x}+\mu\left(\frac{\partial^2 u}{\partial x^2}+\frac{\partial^2 u}{\partial y^2}+\frac{\partial^2 u}{\partial z^2}\right)+\frac{1}{\rho}\left[\frac{\partial(-\rho\overline{u'^2})}{\partial x^2}+\frac{\partial(-\overline{\rho u'v'})}{\partial y^2}+\frac{\partial(-\overline{\rho u'w'})}{\partial z}\right] \quad (2)$$

Model turbulent

The K- ω SST is one of several turbulence models that combine the K- ε and K- ω models. It is well known that the use of the K- ε model is less sensitive in areas far from the wall. However, it is extremely sensitive to the boundary layer in the adverse pressure gradient area near the wall. As a result, the K- ω SST employs the K- ε model in areas far from the wall and the K- ω model in areas close to the wall. Equation 3 depicts the transport equation for K- ω SST.

$$\frac{\partial(\rho\omega)}{\partial t}+div(\rho\omega U)=div\left[\left(\mu+\frac{\mu_1}{\sigma_{\omega,1}}\right)grad(\omega)\right]+\gamma_2\left(2\rho S_{ij}.S_{ij}-\frac{2}{3}\rho\omega\frac{\partial(U)}{\partial x_j}\delta_{ij}\right)-\beta_2\rho\omega^2+2\frac{\rho}{\sigma_{\omega,2}\omega}\frac{\partial k}{\partial x_k}\frac{\partial\omega}{\partial x_k} \quad (3)$$

Parameter analysis VAWT

Coefficient Power (C_P) is a dimensionless number that is used to measure or compare the output power of wind turbines. This C_P value is calculated by dividing the power on the rotor shaft by the freestream power. Where Equation 4 shows the mathematical expression for C_P. M is the moment of the rotor, relative velocity angular for the ω, and U for freestream velocity.

$$C_P=\frac{2.M.\omega}{\rho DHU^3} \quad (4)$$

The coefficient Moment (C_M) is a dimensionless number that represents the ratio of the moment by the rotor to the moment that is available in the freestream. This number is used to compare or determine the working rotor's aerodynamic performance.

$$C_M=\frac{M}{\frac{1}{2}\rho ARU^2} \quad (5)$$

TSR is a dimensionless number that represents the ratio of the tangential speed at the rotor to the incoming freestream speed. This TSR is an important component in the discussion of wind turbines; besides being used in calculating turbine performance and turbine characteristics, this TSR value is used in the Darrieus turbine design [18].

$$TSR = \frac{\omega R}{U} \tag{6}$$

Results and Discussion

To determine the effect of the contra-rotating VAWT Darrieus turbine by comparing the performance of contra-rotating and the performance of single-rotating. The compared performance is the value of C_P and aerodynamic performance can be compared from the value of C_M. After the data is obtained from the simulation and calculated, C_P graphs are obtained for contra-rotating and single-rotating as shown in Figure 4.

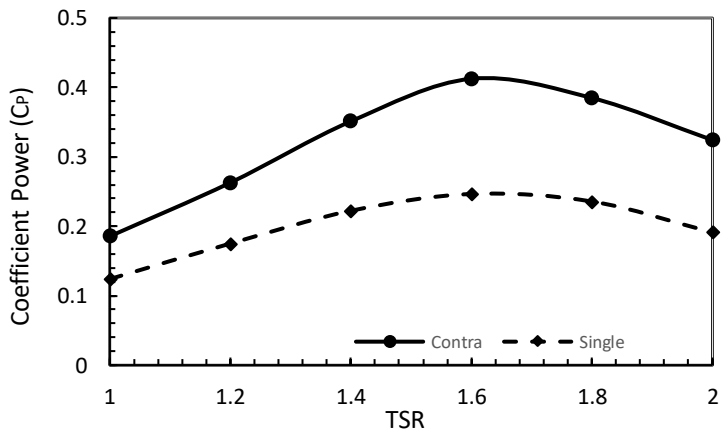

Figure 4: Graph of the change of C_P versus tip speed ratio

From Figure 4 it is known that both contra-rotating and single-rotating have the same peak Cp at TSR 1.6. This shows that although contra-rotating has a higher number of blades than single-rotating which indicates a larger solidity ratio, there should be a different trend of C_P changes to tip speed ratio according to research conducted by [11]. contra-rotating has a total of 6 blades while single-rotating only has 3 blades, it does not change the trend of C_P versus tip speed ratio because in contra-rotating, the addition of the number of blades is not placed on the same rotor so that the solidity remains constant.

The difference in C_P between contra-rotating and single-rotating can be seen clearly in each of the existing tip speed ratios (see Figure 4). The biggest difference lies in tip speed ratio 2 where the difference can reach 70%. This large difference in C_P is mostly due to the difference in angular velocity used, as previously explained that contra-rotating can increase the relative rotational speed.

In this study, the first and second stages have the same tip speed ratio, theoretically, the increase of C_P in contra-rotating can reach 4 times from single-rotating because the relative angular velocity increases up to 2 times [19]. However, the largest increase in C_P contra-rotating only reaches 70%. The loss about 30% of the total increase in C_P from contra-rotating was due to a loss in aerodynamic performance. Figure 5 shows that in terms of aerodynamic performance, single-rotating is superior to contra-rotating for all tip speed ratios.

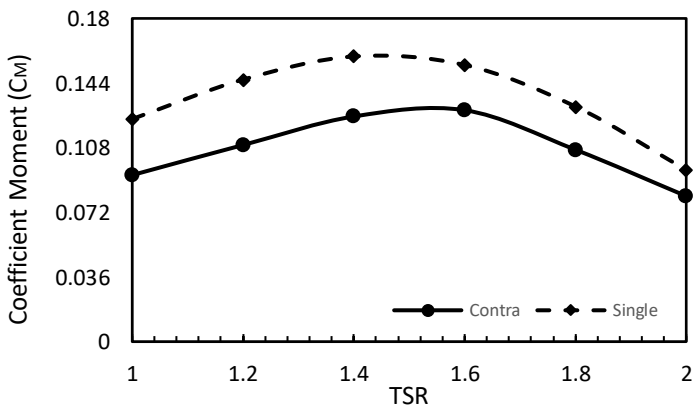

Figure 5: Graph of change in average C_M to tip speed ratio

The greatest reduction in C_M through contra-rotating versus single-rotating was found in tip speed ratio 1 and the smallest was in tip speed ratio 2, with 25% and 15% respectively. Figure 5 depicts the trend of change in C_M versus tip speed ratio, which is identical to the trend of change in C_P to tip speed ratio. Peak C_M differs slightly between single-rotating and contra-rotating, with single-rotating having a C_M of 0.158 at tip speed ratio 1.4 and contra-rotating having a C_M of 0.128 at tip speed ratio 1.6.

The cause of the significant difference in aerodynamic performance between contra-rotating and single-rotating in Figure 5 can be explained in the graph of the change in C_M on the azimuth angle of 1 blade as shown in Figure 6. As an example, the graph C_M as a function of the azimuth angle for one blade is taken at tip speed ratio 1.6 because this tip speed ratio has the largest

different value of C_M between the single-rotating and the contra-rotating. From Figure 6 it can be shown that there is a large difference in the value of C_M when the blade passes through an azimuth angle equal to 90° or at the peak C_M.

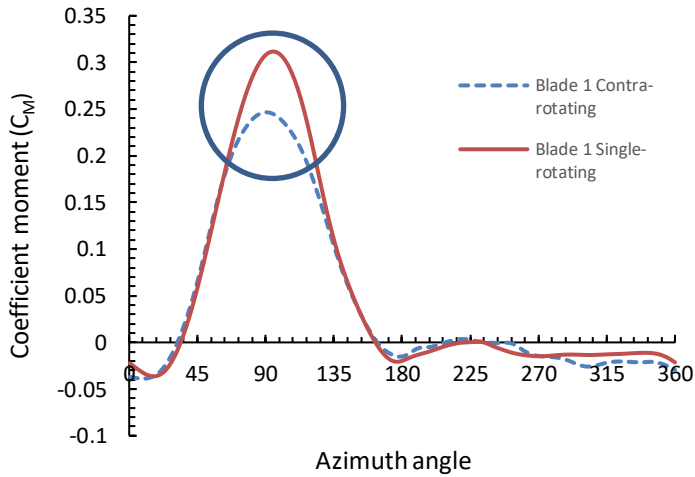

Figure 6: Graph of C_M change to azimuth angle at a tip speed ratio of 1.6

In single-rotating, it is found that the C_M at the azimuth angle of 90° is around 0.31 while in contra-rotating the C_M is 0.246. The difference between the two configurations with the relative ratio is 20%. The difference in the C_M value at the azimuth angle of 90° can occur because there are different aspect ratios for contra-rotating and single-rotating blades, which causes blade tip losses in contra-rotating blades to be greater than for single-rotating blades. Although this study uses the same dimensions between the height of the single-rotating rotor and the combined rotor 1 and 2 in contra-rotating, it does not make the two configurations have the same aspect ratio. This is because rotor 1 and rotor 2 have different rotation directions. When blade 1 on the contra-rotating is at an azimuth angle of 90° or is at the peak C_M, none of the blades on rotor 2 are in the same position as blade 1 on rotor 1.

Figures 7a and 7b for contra-rotating and single-rotating respectively show streamlined pulses at both ends of the blade, indicating a blade phenomenon of tip losses. On the pressure contour, this phenomenon is indicated by a change in the pressure distribution on the low-pressure side from the blade's tip to the center of the blade. The closer the blade tip, the more pressure on the low-pressure side will increase. This is due to the fact that the tip vortex from the high pressure side reduces flow on the low pressure side thus the pressure is increased. In contra-rotating (see Figure 7a), the effect of blade tip losses is strongly marked by an increase in pressure on the low-

pressure side which is almost to the center of the blade due to the small aspect ratio of the blade, while in single-rotating (see Figure 7b), The increase of pressure on the low-pressure side can only be seen around the blade's tip. The closer to the center of the blade, the less noticeable this increase of pressure is. This increase in pressure on the low-pressure side will reduce the difference between the pressure in the high-pressure area and the low-pressure side so that the lift force on the blade is reduced.

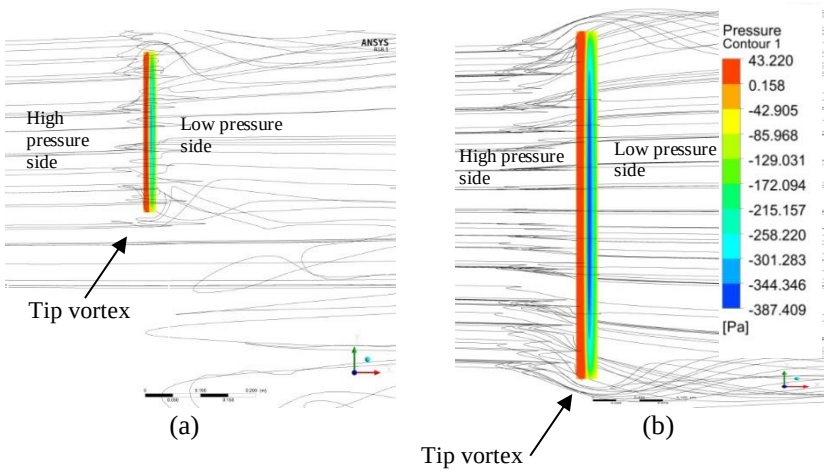

Figure 7: Streamline and contour blade pressure 1 azimuth angle 90º Z view; (a) contra-rotating, and (b) single-rotating

In addition to the effect of blade tip losses due to the difference in aspect ratio between contra-rotating and single-rotating, it is known that the effect of contra-rotating on the VAWT of the Darrieus turbine can be seen in Figure 8. In the graphic image, it is known that there is an increase in C_M in the azimuth angle around 200º-255º for contra-rotating.

The increase in C_M in the azimuth angle 200º-255º is due to the contra-rotating gap between rotor 1 and rotor 2 or what is commonly called the axial distance. In the single-rotating shown in Figure 9b, blade 1 with an azimuth angle position of 200º-255º does not get an additional moment. This is because the flow velocity through blade 1 is the residual velocity from blade 3 with an azimuth angle of 0º-180º. However, in contra-rotating, the freestream velocity through the axial distance formed from blade 3 and blade 4 which forms a straight line parallel to the axial axis does not experience a decrease in velocity due to energy conversion from rotor 1 or rotor 2, so that when the flow flows blade 1 whose position is in the azimuth angle of 200º-255º gets an additional momentum as in Figure 9a and the addition of this momentum can be shown from the larger wake area in Figure 10. It can be seen that the effect of this

axial distance not only increases the momentum around blade 1 but also increases the angle of attack at the azimuth angle of 200º-255º.

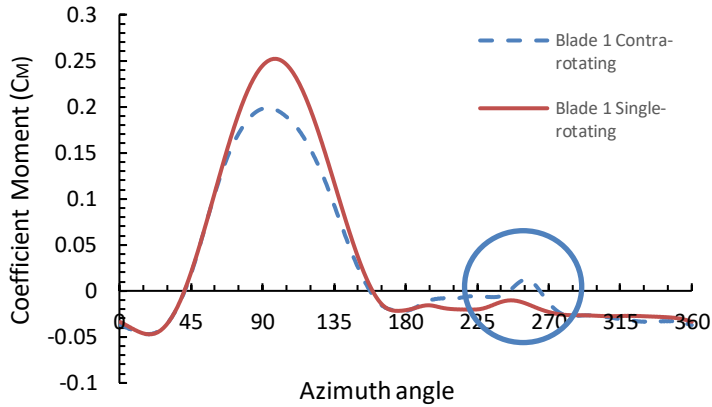

Figure 8: Graph of the change in C_M with respect to the azimuth angle at tip speed ratio 2

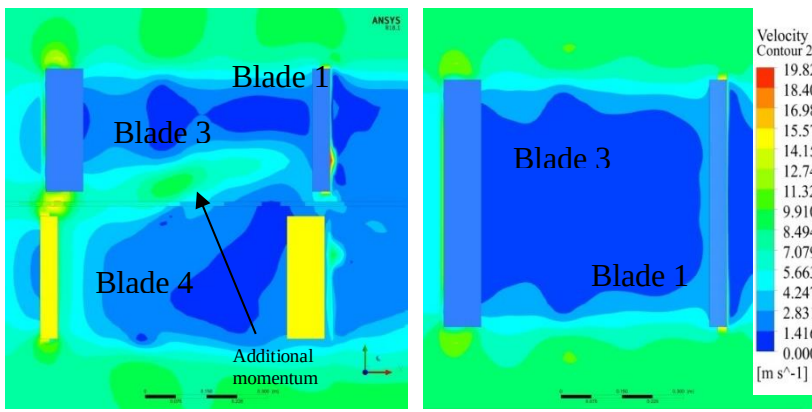

(a) (b)

Figure 9: Absolute velocity contour Z = 0.14 m; (a) contra-rotating, and (b) single-rotating

The contra-rotating moment at the azimuth angle of 200º-255º is still far from the moment produced when blade position 1 is at the optimum azimuth angle or 35º-90º. However, both blade positions receive the same freestream velocity. This is because the moment on the blade is obtained by integrating the tangential force over the entire area of the blade multiplied by the rotor

radius, when the position of blade 1 is at an azimuth angle of 0º-180º, the blade gains moment from the freestream velocity with the same value for the entire area of the blade. When the position of blade 1 is at an azimuth angle of 200º-255º or in a position to obtain additional momentum from the axial distance, not all blade areas receive the additional momentum because some areas on blade 1 receive residual wind or wake from blade 3 (see Figure 9a). Even though the freestream velocity received on blade 1 is the same, the resulting moment generated by blade 1 when it is in position 200º-255º is not as large as when it is in position 35º-90º.

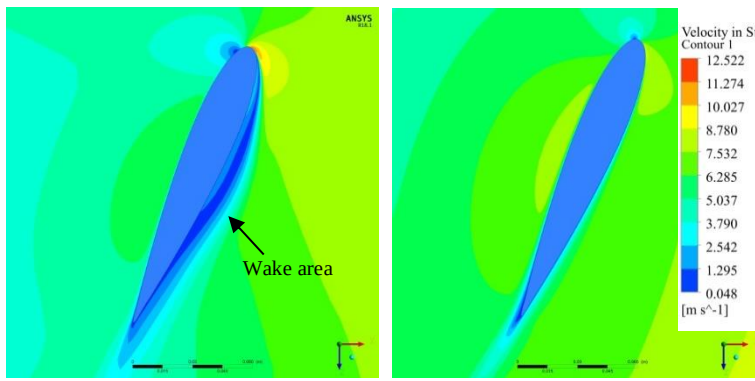

(a) (b)

Figure 10: Relative velocity contour on blade 1 at azimuth angle 247º; (a) contra-rotating, and (b) single-rotating

Conclusion

From this study can be concluded that the contra-rotating configuration on the VAWT Darrieus turbine can increase the C_P of the Darrieus turbine VAWT up to 70% through an increase in the relative rotation of the rotor so that the power generated is greater in all variations of tip speed ratio. However, when viewed through aerodynamic performance or C_M, the contra-rotating configuration of the Darrieus turbine VAWT reduces performance in all variations of tip speed ratio. This is because the blade tip losses in the contra-rotating configuration are greater than the single-rotating due to the different aspect ratios of the two configurations.

The effect of contra-rotating on the VAWT Darrieus turbine can also be seen from C_M when the blade is at an azimuth angle of 200º-255º. There is an increase in C_M due to freestream flow flowing through the axial distance providing fresh air and is known to increase the velocity and the angle of attack of the blade. This axial distance effect is only beneficial for the contra-rotating

VAWT of the Darrieus turbine when the turbine operates at tip speed ratio of 1.6 to tip speed ratio of 2.

The Darrieus contra-rotating configuration is a new configuration that comes with the potential to generate more output power than the conventional Darrieus turbine. The Darrieus turbine VAWT contra-rotating will be better described as a result of this research, mainly its effect on aerodynamic performance. However, further research on the Darrieus contra-rotating VAWT turbine is needed to determine how the aerodynamic performance with axial distance variations and when the aspect ratio between stage 1 and the single-rotating rotor is made the same.

Contributions of Authors

The authors confirm the equal contribution in each part of this work. All authors reviewed and approved the final version of this work.

Funding

This work received no specific grant from any funding agency.

Conflict of Interests

All authors declare that they have no conflicts of interest

Acknowledgment

Special thanks to the staffs and members of fluid mechanic laboratory who always provide facilities that are needed in order to complete this work.

References

[1] M. M. Aslam Bhutta, N. Hayat, A. U. Farooq, Z. Ali, S. R. Jamil, and Z. Hussain, "Vertical axis wind turbine - A review of various configurations and design techniques," *Renewable and Sustainable Energy Reviews*, vol. 16, no. 4, pp. 1926–1939, 2012, doi: 10.1016/j.rser.2011.12.004.

[2] A. Subramanian *et al*., "Effect of airfoil and solidity on performance of small scale vertical axis wind turbine using three dimensional CFD model," *Energy*, vol. 133, pp. 179–190, 2017, doi:

10.1016/j.energy.2017.05.118.

[3] S. Chhin and V. S. Djanali, "Numerical Simulation on Hybrid Savonius Turbine with NACA-Airfoils as H-rotor Blades," *Proceeding-2020 International Seminar on Intelligent Technology and Its Applications ISITIA 2020*, pp. 123–128, 2020, doi: 10.1109/ISITIA49792.2020.9163710.

[4] M. H. Mohamed, "Impacts of solidity and hybrid system in small wind turbines performance," *Energy*, vol. 57, pp. 495–504, 2013, doi: 10.1016/j.energy.2013.06.004.

[5] M. D. Bausas and L. A. M. Danao, "The aerodynamics of a camber-bladed vertical axis wind turbine in unsteady wind," *Energy*, vol. 93, pp. 1155–1164, 2015, doi: 10.1016/j.energy.2015.09.120.

[6] Q. Li, T. Maeda, Y. Kamada, J. Murata, K. Furukawa, and M. Yamamoto, "Effect of number of blades on aerodynamic forces on a straight-bladed Vertical Axis Wind Turbine," *Energy*, vol. 90, pp. 784–795, 2015, doi: 10.1016/j.energy.2015.07.115.

[7] Q. Li *et al.*, "Effect of solidity on aerodynamic forces around straight-bladed vertical axis wind turbine by wind tunnel experiments (depending on number of blades)," *Renewable Energy*, vol. 96, pp. 928–939, 2016, doi: 10.1016/j.renene.2016.05.054.

[8] M. A. Miller, S. Duvvuri, and M. Hultmark, "Solidity effects on the performance of vertical-axis wind turbines," *Flow*, vol. 1, pp. 1–15, 2021, doi: 10.1017/flo.2021.9.

[9] Q. Li *et al.*, "Effect of rotor aspect ratio and solidity on a straight-bladed vertical axis wind turbine in three-dimensional analysis by the panel method," *Energy*, vol. 121, pp. 1–9, 2017, doi: 10.1016/j.energy.2016.12.112.

[10] H. Zhu, W. Hao, C. Li, and Q. Ding, "Numerical study of effect of solidity on vertical axis wind turbine with Gurney flap," *Journal of Wind Engineering and Industrial Aerodynamics*, vol. 186, no. December 2018, pp. 17–31, 2019, doi: 10.1016/j.jweia.2018.12.016.

[11] Q. Liu, W. Miao, C. Li, W. Hao, H. Zhu, and Y. Deng, "Effects of trailing-edge movable flap on aerodynamic performance and noise characteristics of VAWT," *Energy*, vol. 189, pp. 116271, 2019, doi: 10.1016/j.energy.2019.116271.

[12] C. C. Chen and C. H. Kuo, "Effects of pitch angle and blade camber on flow characteristics and performance of small-size Darrieus VAWT," *Journal Visualization*, vol. 16, no. 1, pp. 65–74, 2013, doi: 10.1007/s12650-012-0146-x.

[13] A. Rezaeiha, I. Kalkman, and B. Blocken, "Effect of pitch angle on power performance and aerodynamics of a vertical axis wind turbine," *Applied Energy*, vol. 197, pp. 132–150, 2017, doi: 10.1016/j.apenergy.2017.03.128.

[14] M. Elkhoury, T. Kiwata, and E. Aoun, "Experimental and numerical

investigation of a three-dimensional vertical-axis wind turbine with variable-pitch," *Journal of Wind Engineering and Industrial Aerodynamics*, vol. 139, pp. 111–123, 2015, doi: 10.1016/j.jweia.2015.01.004.

[15] G. Abdalrahman, W. Melek, and F. S. Lien, "Pitch angle control for a small-scale Darrieus vertical axis wind turbine with straight blades (H-Type VAWT)," *Renewable Energy*, vol. 114, pp. 1353–1362, 2017, doi: 10.1016/j.renene.2017.07.068.

[16] Y. Guo, X. Li, L. Sun, Y. Gao, Z. Gao, and L. Chen, "Aerodynamic analysis of a step adjustment method for blade pitch of a VAWT," *Journal of Wind Engineering and Industrial Aerodynamics*, vol. 188, no. February, pp. 90–101, 2019, doi: 10.1016/j.jweia.2019.02.023.

[17] S. N. Ashwindran, A. A. Azizuddin, A. N. Oumer, and A. A. Razak, "An Introductory CFD Analysis Study of Novel Cavity Vane Driven Wind Turbine Blade Design," *Journal of Mechanical Engineering*, vol. 17, no. 3, pp. 55–68, 2020.

[18] D. H. Didane, N. Rosly, M. F. Zulkafli, and S. S. Shamsudin, "Performance evaluation of a novel vertical axis wind turbine with coaxial contra-rotating concept," *Renewable Energy*, vol. 115, no. 2018, pp. 353–361, 2018, doi: 10.1016/j.renene.2017.08.070.

[19] Y. Ahmudiarto, T. Admono, A. Salim, and M. Furqon, "Performance and productivity enhancements on vertical axis wind turbines with a novel multi-stages contra-rotating technique," *International Conference on Sustainable Energy Engineering and Application ICSEEA 2018*, pp. 44–50, 2019, doi: 10.1109/ICSEEA.2018.8627119.

[20] D. H. Didane, S. M. Maksud, M. F. Zulkafli, N. Rosly, S. S. Shamsudin, and A. Khalid, "Performance investigation of a small Savonius-Darrius counter-rotating vertical-axis wind turbine," *International Journal Energy Research*, vol. 44, no. 12, pp. 9309–9316, 2020, doi: 10.1002/er.4874.

[21] D. H. Didane, N. Rosly, M. F. Zulkafli, and S. S. Shamsudin, "Numerical investigation of a novel contra-rotating vertical axis wind turbine," *Sustainable Energy Technologies and Assessments*, vol. 31, no. May 2018, pp. 43–53, 2019, doi: 10.1016/j.seta.2018.11.006.

[22] D. H. Didane, D. Kudam, M. F. Zulkafli, S. Mohd, M. F. M. Batcha, and A. Khalid, "Development and Performance Investigation of a Unique Dual-rotor Savonius-type Counter-rotating Wind Turbine," *International Journal Integrated Engineering*, vol. 13, no. 6, pp. 89–98, 2021, doi: 10.30880/ijie.2021.13.06.008.

[23] S. N. Jung, T. S. No, and K. W. Ryu, "Aerodynamic performance prediction of a 30 kW counter-rotating wind turbine system," *Renewable Energy*, vol. 30, no. 5, pp. 631–644, 2005, doi: 10.1016/j.renene.2004.07.005.

[24] B. Ko, S. Liu, Z. Fang, Y. Ahmudiarto, B. Nugroho, and R. Chin, "Numerical simulation of two-stages contra-rotating vertical axis wind

turbine," *22nd Australasian Fluid Mechanics Conference AFMC2020*, no. December, pp. 3–6, 2020, doi: 10.14264/d1c920e.

[25] A. Eltayesh *et al*., "Effect of wind tunnel blockage on the performance of a horizontal axis wind turbine with different blade number," *Energies*, vol. 12, no. 10, pp. 1–15, 2019, doi: 10.3390/en12101988.

[26] A. Rezaeiha, H. Montazeri, and B. Blocken, "Towards accurate CFD simulations of vertical axis wind turbines at different tip speed ratios and solidities: Guidelines for azimuthal increment, domain size and convergence," *Energy Conversion and Management*, vol. 156, no. September 2017, pp. 301–316, 2018, doi: 10.1016/j.enconman.2017.11.026.

[27] F. Balduzzi, A. Bianchini, R. Maleci, G. Ferrara, and L. Ferrari, "Critical issues in the CFD simulation of Darrieus wind turbines," *Renewable Energy*, vol. 85, pp. 419–435, 2016, doi: 10.1016/j.renene.2015.06.048.

[28] Y. T. Lee and H. C. Lim, "Numerical study of the aerodynamic performance of a 500W Darrieus-type vertical-axis wind turbine," *Renewable Energy*, vol. 83, pp. 407–415, 2015, doi: 10.1016/j.renene.2015.04.043.